Supporting Information

Efficient all-polymer solar cells based on a narrow bandgap polymer acceptor

Zhihong Yin,†[a] Yang Wang,†[a] Qing Guo†[a], Lei Zhu,[b] Haiqin Liu,[c] Jin Fang,[a] Xia Guo,*[a] Feng Liu,[b] Zheng Tang,[c] Maojie Zhang,*[a] and Yongfang Li[ad]

[a]Laboratory of Advanced Optoelectronic Materials, College of Chemistry, Chemical Engineering and Materials Science, Soochow University, Suzhou 215123, China.

E-mail: guoxia@suda.edu.cn; mjzhang@suda.edu.cn

[b]Frontiers Science Center for Transformative Molecules, School of Chemistry and Chemical Engineering, Shanghai Jiao Tong University, Shanghai 200240, P. R. China.

[c]Center for Advanced Low-dimension Materials, State Key Laboratory for Modification of Chemical Fibers and Polymer Materials, College of Materials Science and Engineering, Donghua University, Shanghai 201620, China.

[d]Beijing National Laboratory for Molecular Sciences, CAS Key Laboratory of Organic Solids, Institute of Chemistry, Chinese Academy of Sciences, Beijing 100190, China.

†These authors contributed equally to this work.

Materials

The Compound **1** was synthesized according to the procedure reported in the literatures[1]. The polymer donor **PBDB-T** was purchased from Organtec Ltd. and the 2-((5)6-Bromo-3-oxo-2,3-dihydro-1H-inden-1-ylidene)malononitrile (compound **3**) was purchased from Beijing Huawei Ruike Chemical Co.,Ltd.. The poly[(9,9-bis(3-

((N,N-dimethyl)-N-ethylammonium)-propyl)2,7-fluorene)-alt-2,7-(9,9-dioctylfluorene)] (PFN-Br), perylene-diimide (PDIN) and zirconium acetylacetonate (ZrAcac) was purchased from Organtec Solar Materials Inc. The poly[(9,9-bis(3'-(N,N-dimethyl)ethylammoinium-propyl)-2,7-fluorene)-alt-2,7-(9,9-dioctylfluorene)] (PFN) and (N,N-dimethylamino)propyl naphthalene diimide (NDIN) was purchased from Derthon Optoelectronic Materials Science Technology Co., Ltd.. ZnO nanoparticles were synthesized by hydrolysis and condensation of zinc acetate dihydrate by potassium hydroxide in methanol using a Zn^{2+}: OH^- ratio of 1:1.7 accroding to Weller et al.[2,3] The Other common materials and chemical reagents were purchased from commercial sources and used as received. The **PG1** exhibits a number average molecular weight (M_n) of 14.4 KDa with a polydispersity index (PDI) of 2.0, measured by high temperature gel permeation chromatography (GPC) with 1,2,4-trichlorobenzene as eluent and polystyrene standard at 160 ℃. The other chemicals and solvents were purchased from J&K, Alfa Aesar and TCI Chemical Co. respectively. The monomer **M1**, and polymer **PG1** were synthesized according to Scheme S1.
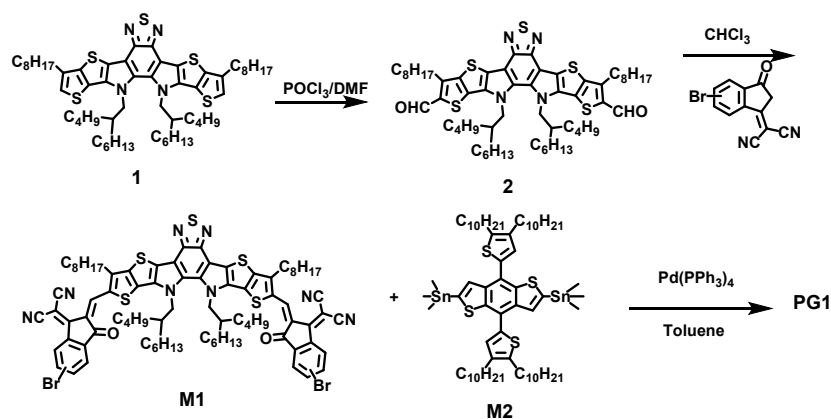
Scheme S1. Synthetic routes for the polymer acceptor PG1.

Synthesis of Compound 2

In a dry round-bottomed flask, compound **1** (640 mg, 0.64 mmol) was dissolved in DMF (50 mL) and placed under a nitrogen atmosphere. The solution was cooled to 0 °C and stirred while phosphorus oxychloride in dichloroethane (0.3 mL, 3.2 mmol) was added dropwise. The mixture was stirred for one hour at 25 °C, and then stirred for five hours at 105 °C. After the reaction, the mixture was cooled to room temperature and poured into ice water. 1 M NaOH solution was added and extracted with dichloromethane, The resulting crude compound was purified by silica gel column using a mixture of hexane/dichloromethane as the eluent to give a yellow solid compound **2** (595 mg, 88%).

Compound 2: ^{1}H NMR (400 MHz, CDCl$_3$) δ 10.13 (s, 2H), 4.63 (d, J = 7.3 Hz, 4H), 3.19 (t, J = 7.6 Hz, 4H), 1.89-1.91 (m, 6H), 1.36-1.44 (m, 4H), 1.16-1.32 (m, 34H), 0.81 (dd, J = 17.4, 10.8 Hz, 18H), 0.49-0.61 (m, 12H). ^{13}C NMR (100 MHz, CDCl$_3$) δ 181.79, 147.49, 146.86, 143.18, 137.04, 136.82, 136.80, 132.95, 129.67, 128.81, 127.43, 127.40, 112.40, 55.28, 31.83, 31.50, 30.34, 30.20, 30.03, 29.64, 29.34, 29.31, 29.18, 28.16, 27.91, 22.73, 22.68, 22.64, 22.43, 22.41, 14.09, 13.94, 13.92, 13.70, 13.67. 13.67. Matrix-Assisted Laser Desorption/Ionization Time of Flight Spectrometry (MALDI-TOF) MS: calculated. For C$_{60}$H$_{86}$N$_4$O$_2$S$_5$ m/z = 1055.54; found, 1055.63.

Synthesis of M1

Compound **2** (0.158 g, 0.15 mmol), 2-((5)6-Bromo-3-oxo-2,3-dihydro-1H-inden-1-ylidene)malononitrile (compound **3** 0.25 g, 0.91 mmol), pyridine (0.5 mL) and chloroform (20 mL) were dissolved in a round bottom flask under nitrogen. The mixture was stirred at 65 °C overnight. After cooling to room temperature, the mixture was poured into methanol and filtered. The residue was purified with column chromatography on silica gel using dichloromethane/petroleum ether (1/1, *v/v*) as the eluent to give a dark blue solid **M1** (0.120 g, 51% yield).

M1: ^{1}H NMR (400 MHz, CDCl$_3$) δ 9.15 (br, 2H), 8.82 (br, 1.2H), 8.55 (br, 0.75H), 8.03 (br, 0.75H), 7.87-7.89 (br, 2H), 7.78-7.80 (br, 1.2H), 4.78 (m, 4H), 3.19-3.23 (t, J = 7.7 Hz, 4H), 2.15 (m, 2H), 1.83-1.89 (m, 4H), 1.47-1.51 (m, 4H), 1.33-1.37 (m, 4H), 1.18-1.33 (m, 32H), 0.87-0.98 (m, 18H), 0.63-0.72 (m, 12H). ^{13}C NMR (100 MHz, CDCl$_3$) δ 187.36, 186.96, 159.85, 159.23, 153.57, 147.45, 145.12, 141.34, 138.49, 138.29, 137.75, 137.69, 137.22, 135.99, 135.94, 135.42, 134.07, 133.48, 130.67, 130.13, 129.47, 128.14, 126.71, 126.34, 124.53, 120.17, 120.09, 115.29, 115.14, 114.91, 114.57, 113.57, 68.81, 68.29, 55.78, 39.22, 31.86, 31.58, 31.20, 30.52, 30.43, 29.85, 29.19, 22.66, 22.53, 22.50, 22.48, 14.11, 14.08, 13.81, 13.77. Matrix-Assisted Laser Desorption/Ionization Time of Flight Spectrometry (MALDI-TOF) MS: calculated. For C$_{84}$H$_{92}$Br$_2$N$_8$O$_2$S$_5$ m/z = 1565.82; found, 1565.43.

Compound 3: ^{1}H NMR (400 MHz, CDCl$_3$) δ 8.76 (s, 0.52H), 7.94-7.96 (d, 0.44H), 7.95 (s, 0.43H), 7.81-7.84 (m, 1H), 7.81-7.82(d, 0.55H), 3.72-3.74 (d, 2H). ^{13}C NMR (100 MHz, CDCl$_3$) δ 193.57, 193.41, 164.99, 164.63, 162.99, 139.15, 138.93, 128.89, 127.96, 127.06, 125.74, 112.05, 111.88, 111.67, 80.43, 79.61, 43.23, 43.19.

Synthesis of PG1

In a 25 mL double-neck round-bottom flask, **M1** (156.6 mg, 0.10 mmol) and (4,8-bis(4,5-didecylthiophen-2-yl)benzo[1,2-b:4,5-*b'*]dithiophene-2,6-diyl)bis(trimethylstannane) (**M2**) (124.1 mg, 0.10 mmol), Pd(PPh$_3$)$_4$ (10 mg), and dry toluene (10 mL) were added. This double-neck round-bottom flask was then charged with N$_2$ cycle technique to 4-remove O$_2$ for three times. The mixture solution was stirred for 5 h at 110 °C under a N$_2$ atmosphere. The highly viscous green solution was cooled down to room temperature. The reaction mixture was precipitated in 200 mL of methanol stirred for 2 h. The crude polymer was collected by filtration and then further purified by Soxhlet extraction with methanol, acetone, hexane, and chloroform, successively. A dark solid was obtained after removing chloroform (145 mg, 62%, M_n = 14.4 kDa, M_w = 26.7 kDa, PDI = 2.0).

Experimental Section

Measurements: ^{1}H NMR and ^{13}C NMR spectra were measured in CDCl$_3$ on Bruker AV 400 MHz FT-NMR spectrometer. UV-vis absorption spectrum was recorded on a UV-Vis-NIR Spectrophotometer of Agilent Technologies Cary Series. The electrochemical cyclic voltammetry (CV) was performed on a Zahner Ennium IM6 Electrochemical Workstation with glassy carbon disk, Pt wire, and Ag/Ag+ electrode as working electrode, counter electrode, and reference electrode respectively, in a 0.1 M tetrabutylammonium hexafluorophosphate (Bu$_4$NPF$_6$) acetonitrile solution. The molecular weights of the polymers were measured by the GPC method with polystyrene as the standard and 1,2,4-trichlorobenzene as the solvent at 160 °C using

Agilent Technologies PL-GPC220. Thermogravimetric analysis (TGA) was measured on TGA/DSC $^{3+}$ from METTLER TOLEDO at a heating rate of 20°C min^{-1} under a nitrogen atmosphere. Differential scanning calorimetry (DSC) was performed on a TA DSC Q-200 with the scan rate of 5°C min^{-1}. Atomic force microscopy (AFM) measurements were performed on a Dimension 3100 (Veeco) Atomic Force Microscope in the tapping mode. Transmission electron microscopy (TEM) was performed using a TePNai G2 F20 S-TWIN instrument at 200 kV accelerating voltage, in which the blend films were prepared using a processing technique, as following: first, the **PBDB-T:PG1** films were spin-cast on the ITO/PEDOT:PSS substrates, and then the resulting substrates with the **PBDB-T:PG1** films were submerged in deionized water to make these **PBDB-T:PG1** films float onto the water/air interface, and finally the floated **PBDB-T:PG1** films were picked up on unsupported 200 mesh copper grids. The GIWAXS measurements were performed at beamline 7.3.3 at the Advanced Light Source (ALS). Samples were prepared on a Si substrate under the same conditions as those used for device fabrication. The 10 KeV X-ray beam was incident at a grazing angle of 0.11°-0.15°, which maximized the scattering intensity from the samples. The scattered x-rays were detected using a Dectris Pilatus 2M photon counting detector. The crystal coherence length (CCL) was defined as CCL = 0.9 ×(2π/FWHM) (Å), where FWHM is the full width at half maximum of the corresponding diffraction peak.

Fabrication and characterization of all-polymer solar cells.

The all-PSC devices structure was ITO/PEDOT:PSS/active layer/ZnO/Al. In an

ultrasonic bath, the ITO-coated glass (15 Ω/sq) was cleaned with deionized water, acetone and isopropanol. After UVO cleaning for 10 min, and then a 30 nm thick poly(3,4-ethylenedioxythiophene):poly(styrenesulfonate) (PEDOT:PSS) (Bayer Baytron 4083) anode buffer layer was spin-cast onto the ITO substrate and then dried by baking in an oven at 150 °C for 15 min. In a nitrogen glove box, the active layers were then deposited atop the PEDOT:PSS layer by spin-coating a CF solution of **PBDB-T:PG1** (1.5:1, w:w) with a blend concentration of 14 mg/mL. The thickness of the active layers was about 100 nm and controlled by adjusting the spin speed during the spincoating process and measured by a KLA Tencor D-100 profilometer. The ZnO nanoparticle (ZnO NPs) was then deposited on top of the active layers. The PFN-Br was deposited on top of the active layers by spin-coating an methanol solution with a concentration of 0.2 mg/mL under 3000 rpm for 30 s. The PDIN was soluble in methanol containing a small amount of acetic acid (about 0.1% in volume) solution with a concentration of 1.5 mg/mL were then deposited atop the active layer at 3000 rpm for 30 s. The ZrAcac was deposited on top of the active layers by spin-coating an ethanol solution with a concentration of 0.5 mg/mL under 3000 rpm for 30 s. The PDINO was deposited on top of the active layers by spin-coating a methanol solution with a concentration of 1 mg/mL under 3000 rpm for 30 s. The PFN was soluble in methanol containing a small amount of acetic acid (about 0.4% in volume) solution with a concentration of 1.5 mg/mL were then deposited atop the active layer at 3000 rpm for 30 s. The NDIN was soluble in methanol containing a small amount of acetic acid (about 0.1% in volume) solution with a concentration of 0.5 mg/mL

were then deposited atop the active layer at 3000 rpm for 30 s. Finally, 100 nm Al was evaporated under vacuum at a pressure of *ca*. 4×10^{-4} Pa, and through a shadow mask to determine the active area of the devices ($\sim 2 \times 2$ mm^2). The PCE values of the PSCs were measured under an illumination of AM 1.5G (100 mW/cm^2) using a SS-F5-3A solar simulator (AAA grade, 50×50 mm^2 photobeam size) of Enli Technology CO, Ltd. A 2×2 cm^2 monocrystalline silicon reference cell (SRC-00019) was purchased from Enli Technology CO., Ltd. PCE statistics were obtained using 10 individual devices fabricated under the same conditions. The EQE was measured by Solar Cell Spectral Response Measurement System QE-R3011 (Enli Technology CO., Ltd.). The light intensity at each wavelength was calibrated with a standard single crystal Si photovoltaic cell. Sensentive EQE measurements were done using a chopped monochromatic light source (chopping frequency 173 Hz), a current preamplifier (Stanford Instrument, SR570), a lock-in amplifier (Stanford Instrument, SR830), a reference Si diode. EQE-EL measurements were done using a home built setup. In this measurment, electric current was injected into the solar cell by a forward voltage bias, using a Keithly 2400 source meter, and emission from the solar cell was recorded by a Si diode and a Keithly picoammeter. The light intensity at each wavelength was calibrated with a standard single-crystal Si photovoltaic cell.

Mobility measurement

Hole and electron mobility were measured using the space-charge limited current (SCLC) method. Device structures are ITO/PEDOT:PSS/Active layer/MoO$_3$/Al for

hole-only devices and ITO/ZnO-gel /Active layer/ZnO-NPs/Al for electron-only devices. The SCLC is described by:

$$J = 9\varepsilon_0\varepsilon_r\mu(V_{appl} - V_{bi} - V_s)^2/8L^3$$

Where J is the current density, ε_0 is the permittivity of free space (8.85×10^{-12} F m^{-1}), ε_r is the relative permittivity of the material (assumed to be 3), μ is the mobility of hole or electron, V_{appl} is the applied voltage, V_{bi} is the built-in voltage, V_s is the voltage drop from the substrate's series resistance (V_s = IR) and L is the thickness of the active layer.
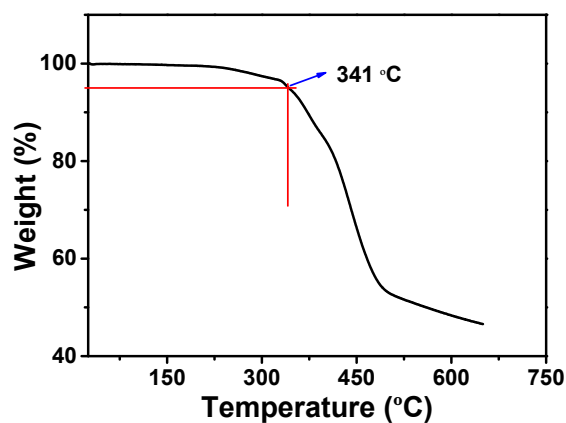
Fig. S1 The TGA curve of PG1 at a scan rate of 20 °C min^{-1} under nitrogen.
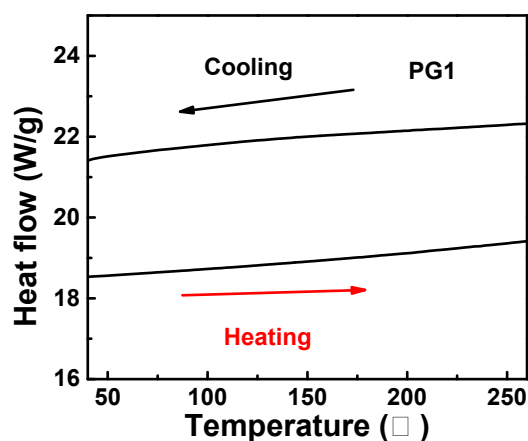
Fig. S2 DSC curves of PG1 at a scan rate of 5 °C min^{-1} under nitrogen.
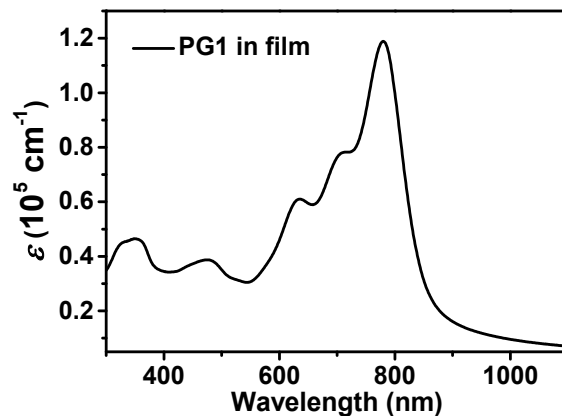
Fig. S3 The UV-vis absorption spectra of PG1 in thin solid films.
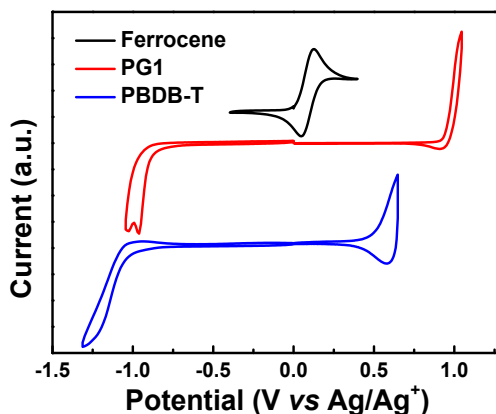
Fig. S4 Cyclic voltammetry of PG1 and PBDB-T films on a glassy carbon electrode

measured in a 0.1 mol/L Bu_4NPF_6 acetonitrile solution at a scan rate of 20 mV/s.
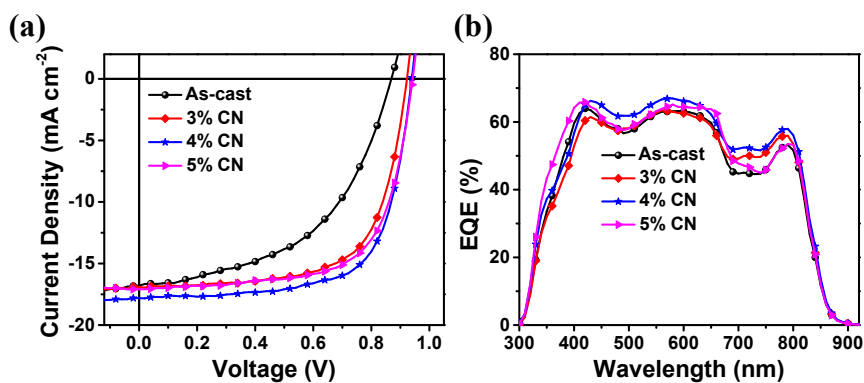
Fig. S5 The *J-V* and (b) EQE characteristics of the all-PSCs based on PBDB-T:PG1

(1.5:1, w/w) with different contents of CN under the illumination of AM 1.5G, 100

mW cm^{-2}.

Table S1. Photovoltaic parameters of all-PSCs based on PBDB-T:PG1 (1.5:1, w/w) with different concentration of CN additive.

Conditions	Speeds (rpm)	V_{oc} (V)	J_{sc}[a] (mA cm^{-2})	FF	PCE[b] (%)
As-cast	3000	0.87 (0.86±0.01)	16.8 (16.4)	0.51 (0.50±0.01)	7.5 (7.3±0.2)
3% CN	3300	0.92 (0.90±0.02)	16.9 (16.5)	0.67 (0.65±0.02)	10.4 (10.2±0.2)
4% CN	3000	0.94 (0.93±0.01)	17.8 (17.5)	0.69 (0.68±0.01)	11.5 (11.3±0.2)
5% CN	3500	0.94 (0.93±0.01)	17.1 (16.8)	0.67 (0.66±0.01)	10.8 (10.5±0.3)

[a] The integral J_{sc} in parentheses from the EQE curves. [b] The average PCE in parentheses from more than 10 devices.
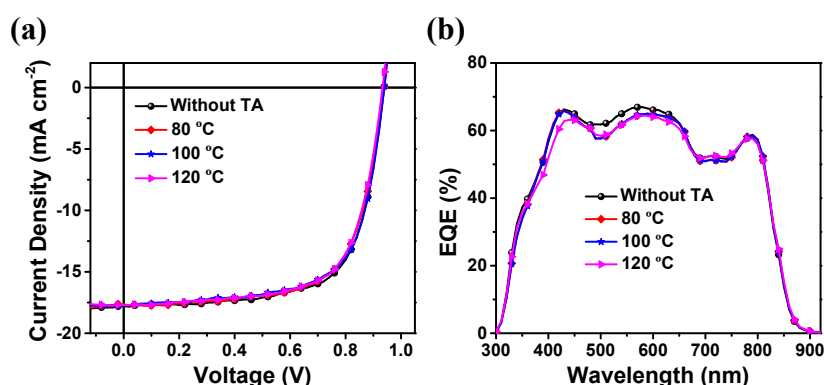
Fig. S6 The *J-V* and (b) EQE characteristics of the all-PSCs based on PBDB-T:PG1 (1.5:1, w/w) with 4% CN at different annealing temperature for 5 min under the illumination of AM 1.5G, 100 mW cm^{-2}.

Table S2. Photovoltaic parameters of all-PSCs based on PBDB-T:PG1 (1.5:1, w/w) with 4% CN at different annealing temperature for 5 min under the illumination of AM 1.5G, 100 mW cm^{-2}.

Conditions	Speeds	V_{oc}	J_{sc}[a]	FF	PCE[b]

	(rpm)	(V)	(mA cm^{-2})		(%)
Without TA	3000	0.94 (0.93±0.01)	17.8 (17.5)	0.69 (0.68±0.01)	11.5 (11.3±0.2)
80 ℃	3200	0.94 (0.93±0.01)	17.7 (17.2)	0.68 (0.66±0.02)	11.3 (11.1±0.2)
100 ℃	3400	0.94 (0.92±0.02)	17.7 (17.2)	0.68 (0.65±0.03)	11.3 (11.1±0.2)
120 ℃	3500	0.94 (0.92±0.02)	17.5(17.1)	0.68 (0.65±0.03)	11.2 (11.0±0.2)

[a] The integral J_{sc} in parentheses from the EQE curves. [b] The average PCE in parentheses from more than 10 devices.
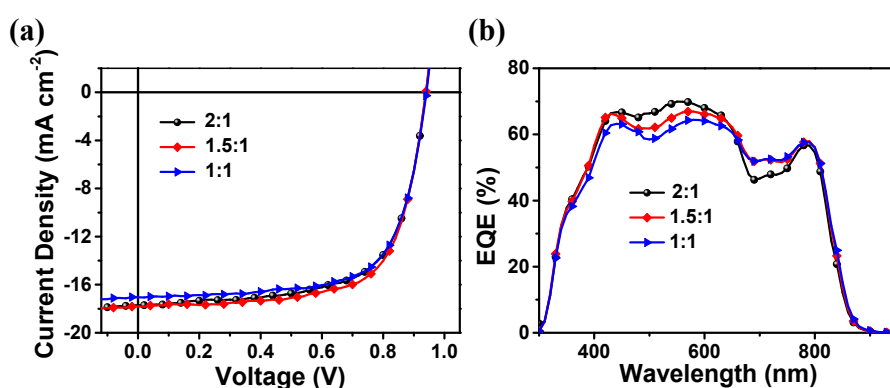
Fig. S7 The *J-V* and (b) EQE characteristics of the all-PSCs based on PBDB-T:PG1 at different D/A weight ratios with contents of 4% CN under the illumination of AM 1.5G, 100 mW cm^{-2}.

Table S3. Photovoltaic parameters of the all-PSCs based on PBDB-T:PG1 at different D/A weight ratios with 4% CN under the illumination of AM 1.5G, 100 mW cm^{-2}.

D/A (w/w)	Speeds (rpm)	V_{oc} (V)	J_{sc}[a] (mA cm^{-2})	FF	PCE[b] (%)
2:1	3200	0.94 (0.93±0.01)	17.7 (17.5)	0.66 (0.64±0.02)	11.0 (10.7±0.3)
1.5:1	3000	0.94 (0.93±0.01)	17.8 (17.5)	0.69 (0.68±0.01)	11.5 (11.3±0.2)
1:1	3500	0.94 (0.93±0.01)	17.3(17.1)	0.68 (0.67±0.01)	11.1 (10.9±0.2)

[a] The integral J_{sc} in parentheses from the EQE curves. [b] The average PCE in parentheses from more than 15 devices.
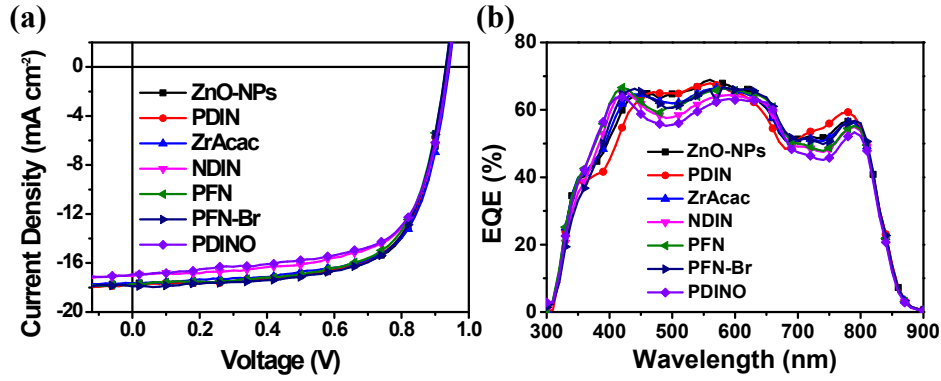
Fig. S8. The *J-V* curves of the PBDB-T:PG1 (1.5:1, w/w)-based all-PSCs with 4% CN at different electron transporting layers (ETLs) under the illumination of AM 1.5G, 100 mW cm^{-2}. Various electron transporting layers (ETLs) were used, including ZnO-NPs, PDIN, ZrAcac, NDIN, PFN, PFN-Br, and PDINO.

Table S4. Photovoltaic parameters of the PBDB-T:PG1 (1.5:1, w/w)-based all-PSCs with 4% CN at different electron transporting layers (ETLs) under the illumination of AM 1.5G, 100 mW cm^{-2}. Various electron transporting layers (ETLs) were used, including ZnO-NPs, PDIN, ZrAcac, NDIN, PFN, PFN-Br, and PDINO.

Interface layer	Speeds (rpm)	V_{oc} (V)	J_{sc}[a] (mA cm^{-2})	FF	PCE[b] (%)
ZnO-NPs	3000	0.94 (0.93±0.01)	17.6(17.5)	0.69 (0.68±0.01)	11.5 (11.3±0.2)
PDIN	3300	0.93 (0.92±0.01)	17.8(17.3)	0.68 (0.66±0.02)	11.3 (11.1±0.2)
ZrAcac	3200	0.94 (0.92±0.02)	17.7(17.3)	0.68 (0.65±0.03)	11.3 (11.1±0.2)
NDIN	3600	0.94 (0.93±0.01)	17.1(16.8)	0.67 (0.65±0.02)	10.7 (10.5±0.2)
PFN	3800	0.93 (0.92±0.01)	17.7(17.2)	0.67 (0.64±0.03)	11.1 (10.8±0.3)
PFN-Br	4200	0.93 (0.92±0.01)	17.9(17.4)	0.68 (0.65±0.03)	11.4 (11.1±0.3)
PDINO	3500	0.94 (0.92±0.02)	16.9(16.4)	0.67 (0.65±0.02)	10.6 (10.4±0.2)

[a] The integral J_{sc} in parentheses from the EQE curves. [b] The average PCE in parentheses from more than 15 devices.
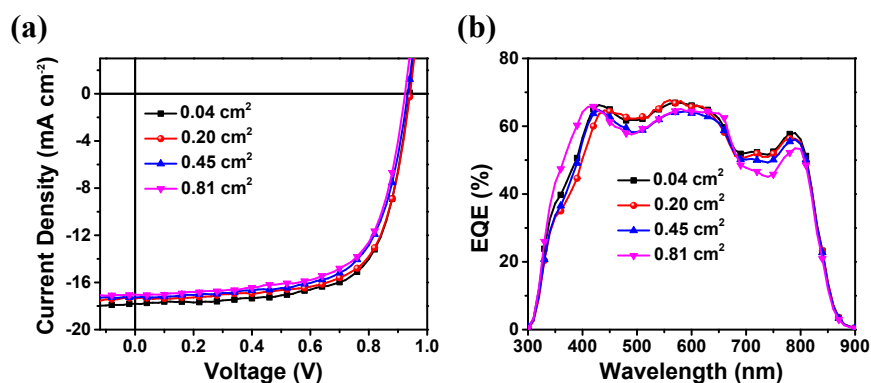
Fig. S9 The *J-V* and (b) EQE characteristics of the all-PSCs based on PBDB-T:PG1 (1.5:1, w/w) with 4% CN at different active area under the illumination of AM 1.5G, 100 mW cm^{-2}.

Table S5. Photovoltaic parameters of the PBDB-T:PG1 (1.5:1, w/w)-based PSCs with 4% CN at different active area under the illumination of AM 1.5G, 100 mW cm^{-2}.

Area (cm^2)	Speeds (rpm)	V_{oc} (V)	J_{sc}[a] (mA cm^{-2})	FF	PCE[b] (%)
0.04	3000	0.94 (0.93±0.01)	17.8 (17.5)	0.69 (0.68±0.01)	11.5 (11.3±0.2)
0.20	3500	0.94 (0.93±0.01)	17.4 (17.3)	0.69 (0.67±0.02)	11.3 (11.0±0.3)
0.45	3800	0.93 (0.92±0.01)	17.3 (16.9)	0.67 (0.66±0.01)	10.8 (10.6±0.2)
0.81	3500	0.92 (0.90±0.02)	17.0 (16.8)	0.67 (0.65±0.02)	10.6 (10.3±0.3)

[a] The integral J_{sc} in parentheses from the EQE curves. [b] The average PCE in parentheses from more than 15 devices.
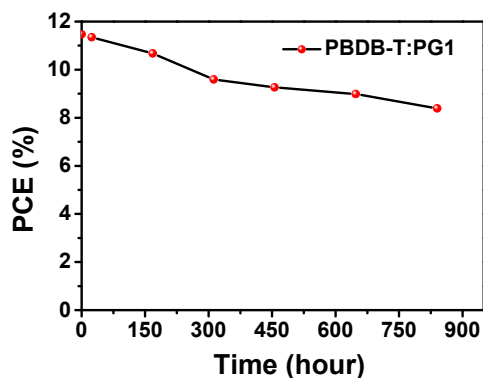
Fig. S10 Storage stability (in the N$_2$-filled glovebox) of the PBDB-T:PG1device.
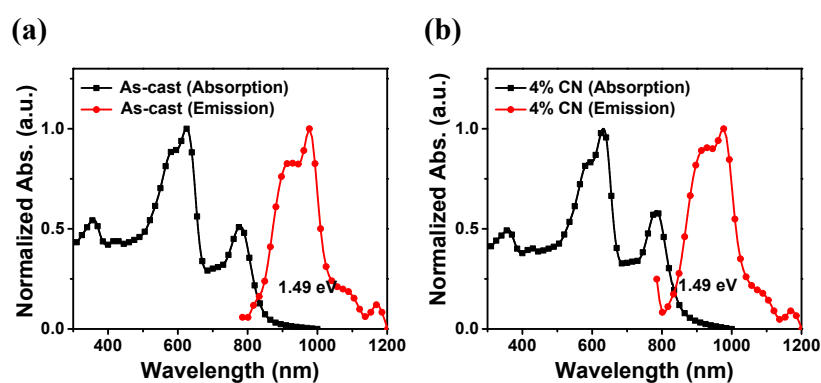
Fig. S11 Normalized absorption spectra and emission spectra of (a) the as cast PBDB-T:PG1 and (b) the 4% CN PBDB-T:PG1.
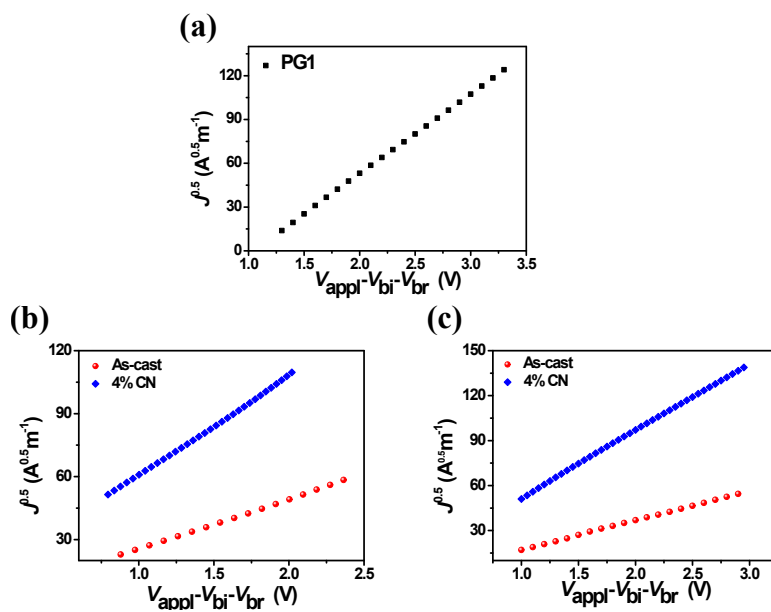
Fig. S12 $J^{1/2}$-V plots of (a) the PG1 pure film, (b) hole-only and (c) the electron-only devices based on PBDB-T: PG1 blends without and with CN treatment.

Table S6. Summarized hole and electron mobilities (μ_h and μ_e) of the device active layers measured by SCLC method.

Condition	μ_h(10^{-4} cm$^2 \cdot$V$^{-1} \cdot$s^{-1})[a]	μ_e(10^{-4} cm$^2 \cdot$V$^{-1} \cdot$s^{-1})[a]	μ_h/μ_e
Pure PG1		8.93±0.13	
As-cast	1.90±0.17	1.01±0.19	1.88±0.18
4% CN	6.76±0.23	6.49±0.22	1.04±0.22

[a] Average values with standard deviations were obtained from 10 devices.

Table S7. Summarized lamellar distance, π-π distance and crystal coherence length of PBDB-T and PG1-based neat and blended films from GIWAXS.

	In plane	Out of plane	Crystal coherence length	
	d-spacing(Å)	π-π(Å)	$L_{c\text{-}100,IP}$(Å)	$L_{c\text{-}010,OOP}$(Å)
PBDB-T	20.9	3.67	80.9	29.2
PG1	19.6	3.85	82.9	17.8
As-cast	20.9	3.82	92.8	15.1
4% CN	21.1	3.71	199.2	28.3
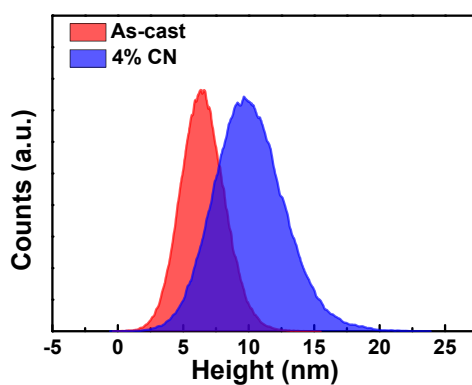
Fig. S13 Surface height histograms extracted from the AFM images in the blend without CN treatment and the blend with 4% CN additive treatment.

Reference

[1] J. Yuan, Y. Zhang, L. Zhou, G. Zhang, H.-L.Yip, T.-K. Lau, X. Lu, C. Zhu, H. Peng, P. A. Johnson, M. Leclerc, Y. Cao, J. Ulanski, Y. Li, Y. Zou, *Joule*, 2019, **3**, 1140.

[2] C. Pacholski, A. Kornowski, H. Weller, *Angew. Chem., Int. Ed.* 2002, **41**, 1188.

[3] W. J. E. Beek, M. M. Wienk, M. Kemerink, X. Yang and R. A. J. Janssen, *J. Phys. Chem. B* 2005, **109**, 9505.